

# Shielding of Quadrupoles from Fringe Field of Target Magnet

Bob Weggel, Particle Beam Lasers, Inc.  
June 24, 2013

Figure 1 plots the on-axis field upstream, from  $-15$  m to zero, of a Target Magnet whose field downstream ramps from  $15$  T to  $1.5$  T at  $z = 5$  m beyond the downstream end of the target region. Figure 2 plots the field magnitude off-axis over the range  $-12 < z < 2$  m,  $0 < r < 8$  m.

On-Axis Field Profile of Target Magnet 15to1.5T5m1+5 of 6/18/2013

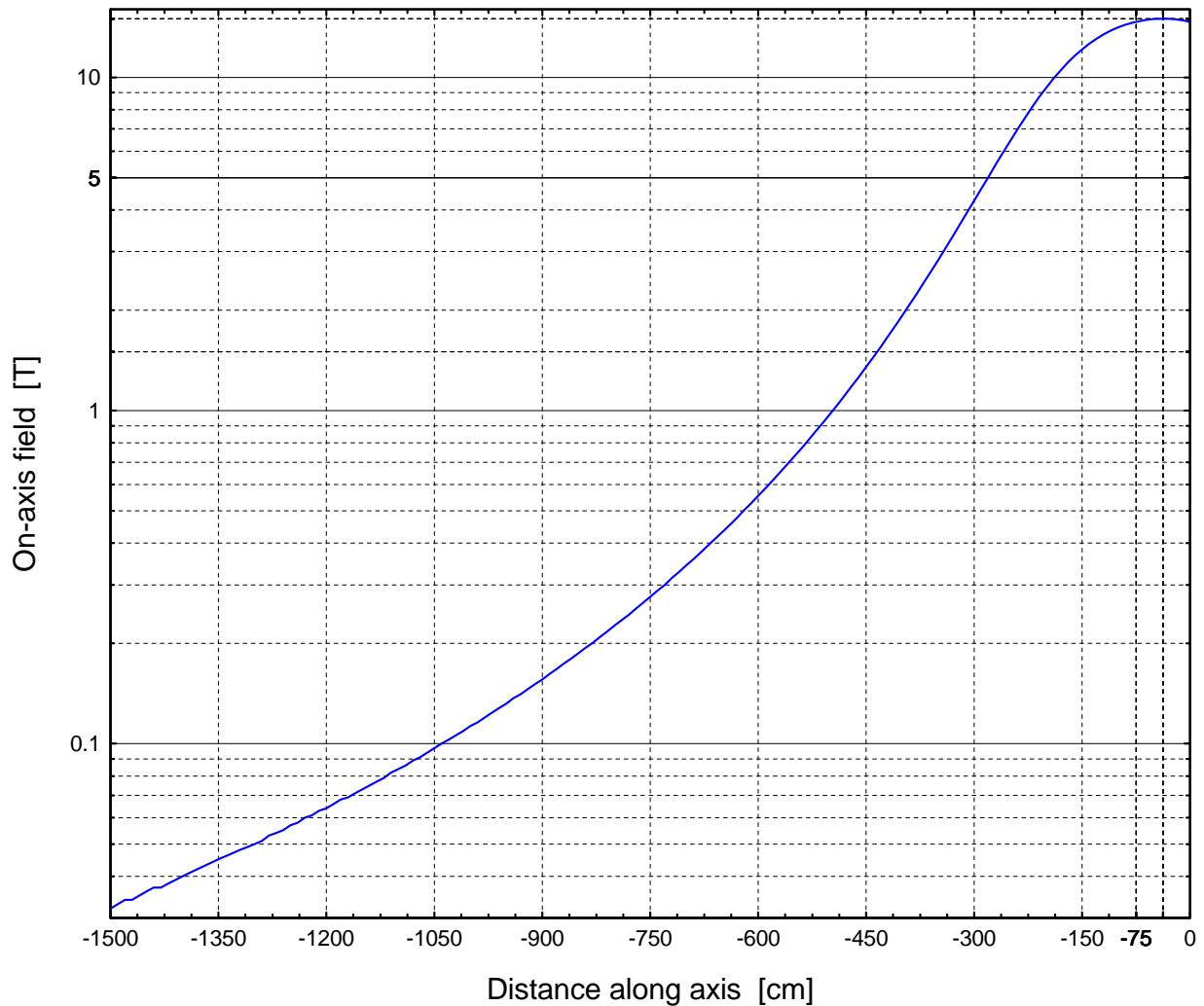


Fig. 1. On-axis field upstream of  $z = 0$  of Target Magnet that ramps from  $15$  T at  $z = -37.5$  cm to  $1.5$  T at  $500$  cm.  
 $B(z) \approx 0.032$  T at  $z = -15$  m,  $0.1$  T at  $z \approx -10.5$  m &  $1$  T at  $z \approx -5$  m.

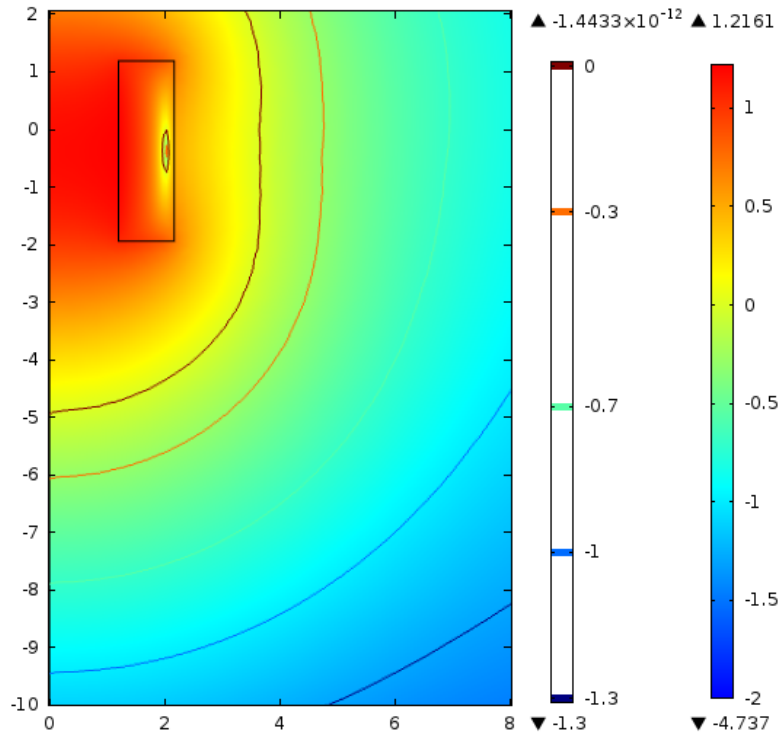


Fig. 2.  $\text{Log}_{10}$  of field  $|B|$  [in teslas] of Target Magnet. Contours are [ $10^{-1.3} \approx 0.05$  (navy), 0.1, 0.2, 0.5, 1 (maroon)].

Figures 3a-d plot the field with an annular disc of soft iron with inner radius of 0.3 m and outer radius of either 3 m, 4 m, 5 m or 6 m; the corresponding disc thicknesses, to avoid saturation, are [60, 80, 100, 120] cm. The respective masses are [131, 312, 610, 1056] metric tonnes.

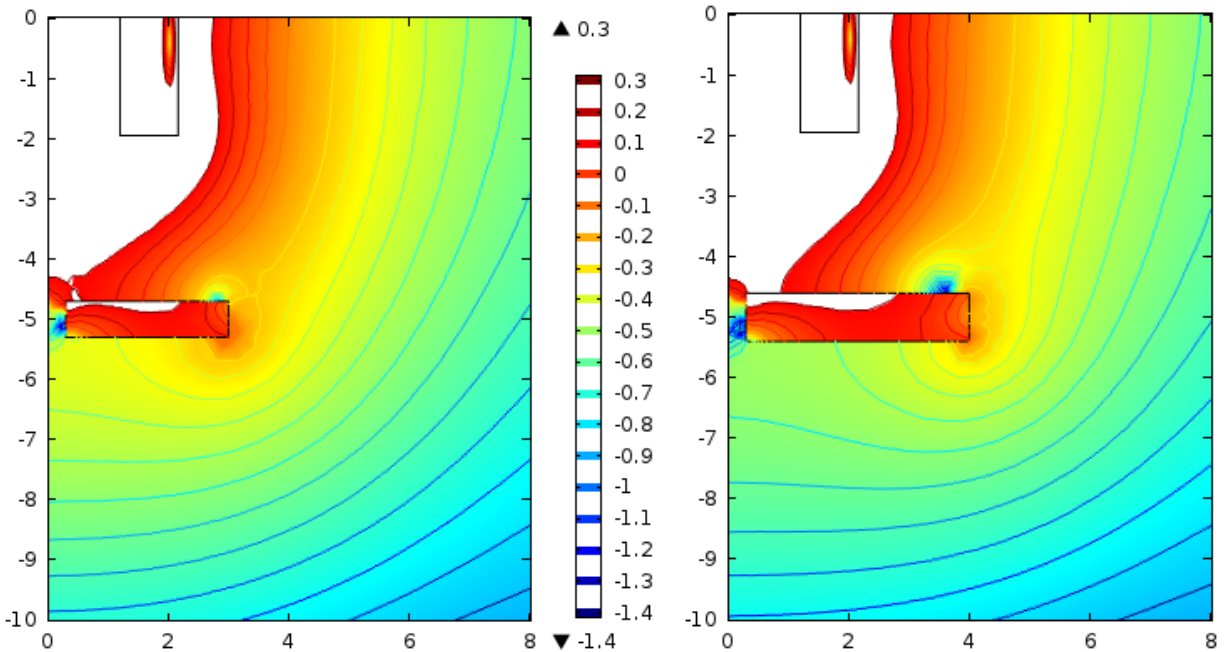


Fig. 3a&b. Field with annular iron disc of 30-cm I.R.; in white areas,  $B > 2$  T. Left: O.R.= 3 m;  $t = 60$  cm;  $M = 131$  metric tonnes. Contours are [ $10^{-1.4} \approx 0.04$  (navy), 0.05, 0.063, 0.08, 0.1, 0.126, 0.16, 0.2, 0.25, 0.32, 0.4, 0.5, 0.63, 0.8, 1, 1.26, 1.6, 2 (maroon)]. Right: O.R.= 4 m;  $t = 80$  cm;  $M = 312$  tonnes.

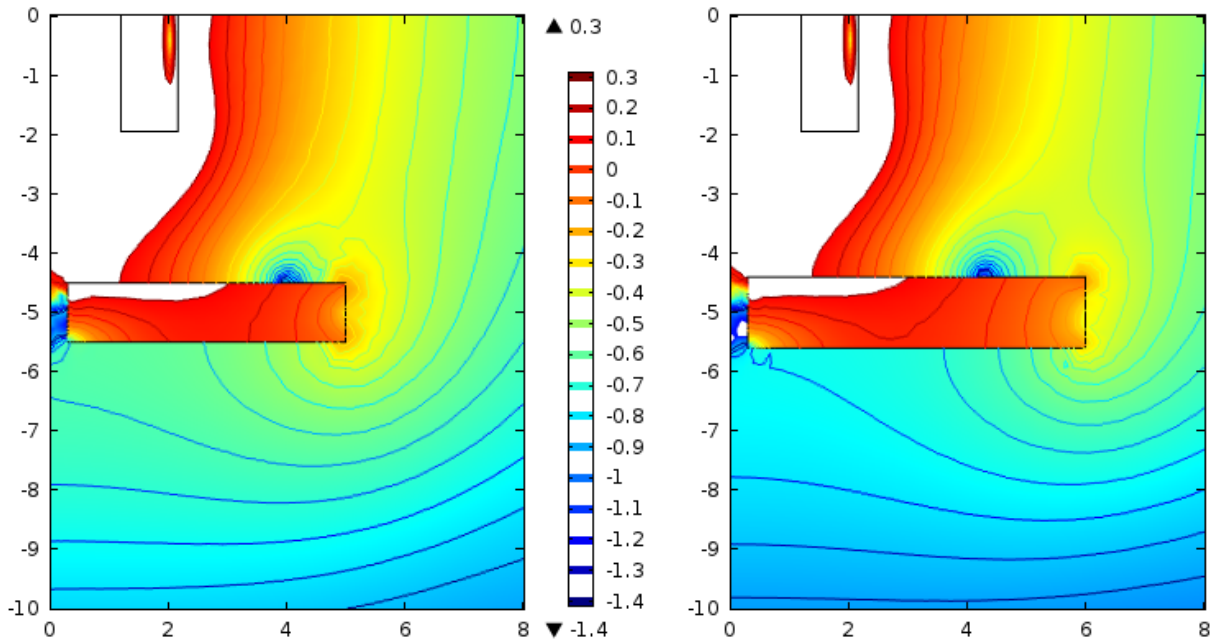


Fig. 3c&d.  $\text{Log}_{10}$  of field with annular disc of 30-cm I.R. Left: O.R. = 5 m;  $t = 100$  cm;  $M = 610$  tonnes. Right: O.R. = 6 m;  $t = 120$  cm;  $M = 1056$  tonnes.

Figures 4a&b plot the field with shielding in the form of a cylindrical shell of 1-m I.R. In Fig. 4a the length is 3 m, the thickness is 80 cm, and the mass is 165 tonnes. In Fig. 4b,  $L = 4$  m,  $t = 100$  cm and  $M = 294$  tonnes. The shielding is globally worse but locally much better than with an annular disc.

Figure 5 shows that adding an upstream flange greatly reduces the field penetration into the upstream mouth of the cylinder.

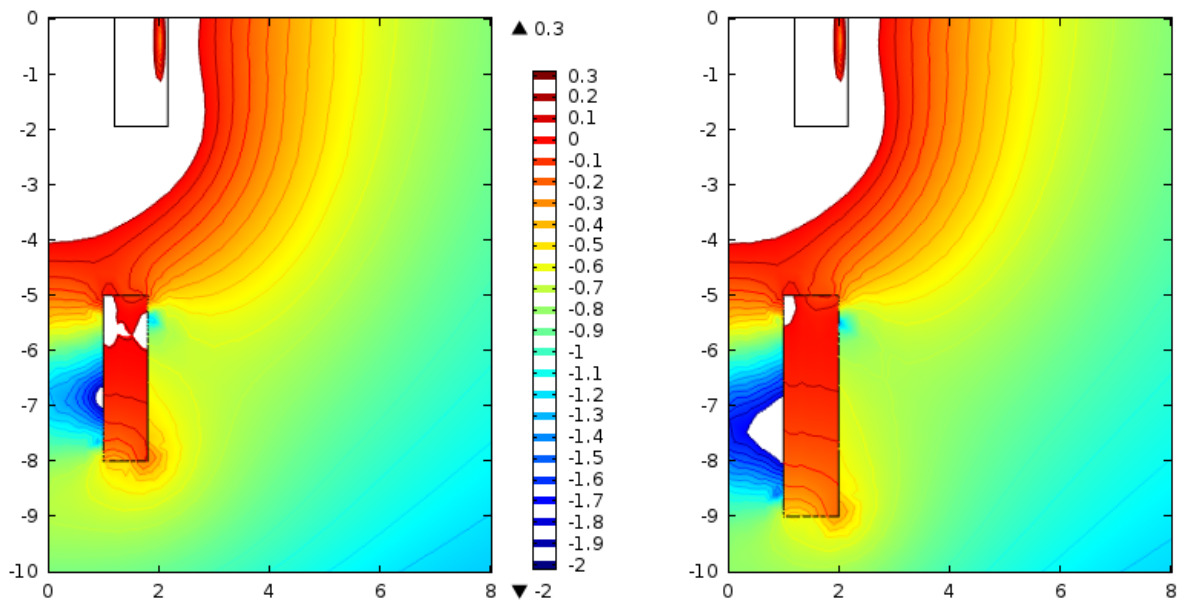


Fig. 4a&b.  $\text{Log}_{10}$  of field with thick-walled cylinder of 1-m I.R. Left:  $L = 3$  m;  $t = 80$  cm;  $M = 165$  tonnes. Right:  $L = 4$  m;  $t = 100$  cm;  $M = 294$  tonnes.

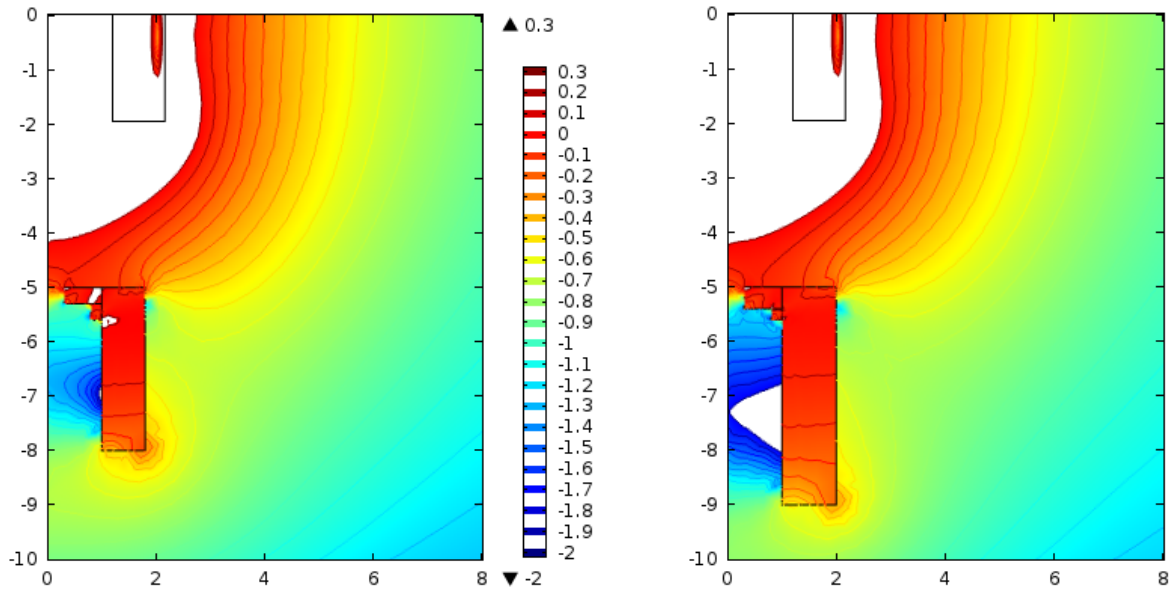


Fig. 5a&b.  $\text{Log}_{10}$  of field with cylindrical shell of 1-m I.R. & upstream flange of 0.3-m I.R. Left:  $L = 3$  m;  $t = 80$  cm;  $M \approx 171$  tonnes. Right:  $L = 4$  m;  $t = 100$  cm;  $M \approx 303$  tonnes.

Figure 6 demonstrates the improvement in shielding quality and cost of shrinking the I.R. of the cylinder from 100 cm to 60 cm and of the flange from 30 cm to 15 cm.

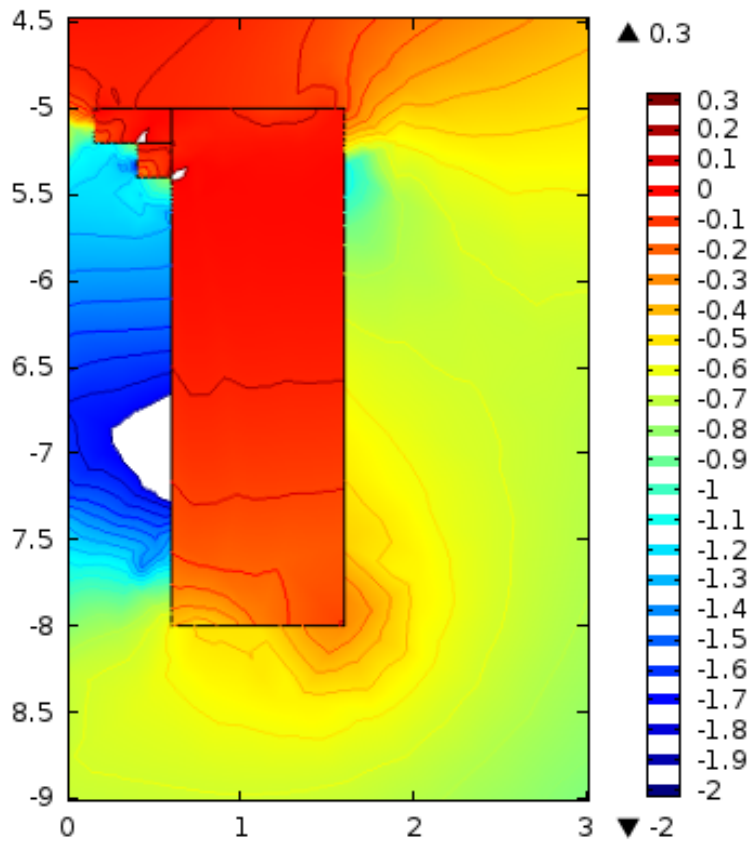


Fig. 6.  $\text{Log}_{10}$  of field with cylindrical shell of 0.6-m I.R., 3-m length & 100-cm thickness, with flange of 15-cm I.R.;  $M \approx 163$  tonnes.

Figure 7 plots the field of a shielding shell much like that of Fig. 6 but with the complexity (no longer rotationally symmetric) required by the actual Target-Magnet system. The center of the upstream endplane of the cylinder is 1 m from the axis of the Target Magnet, and the cylinder axis has been tipped clockwise to continue to aim at  $r = 0, z = 0$ . I.R. = 60 cm;  $L = 3$  m;  $t = 90$  cm; I.R.' = 15 cm;  $L' = 30$  cm;  $M = 141$  tonnes.

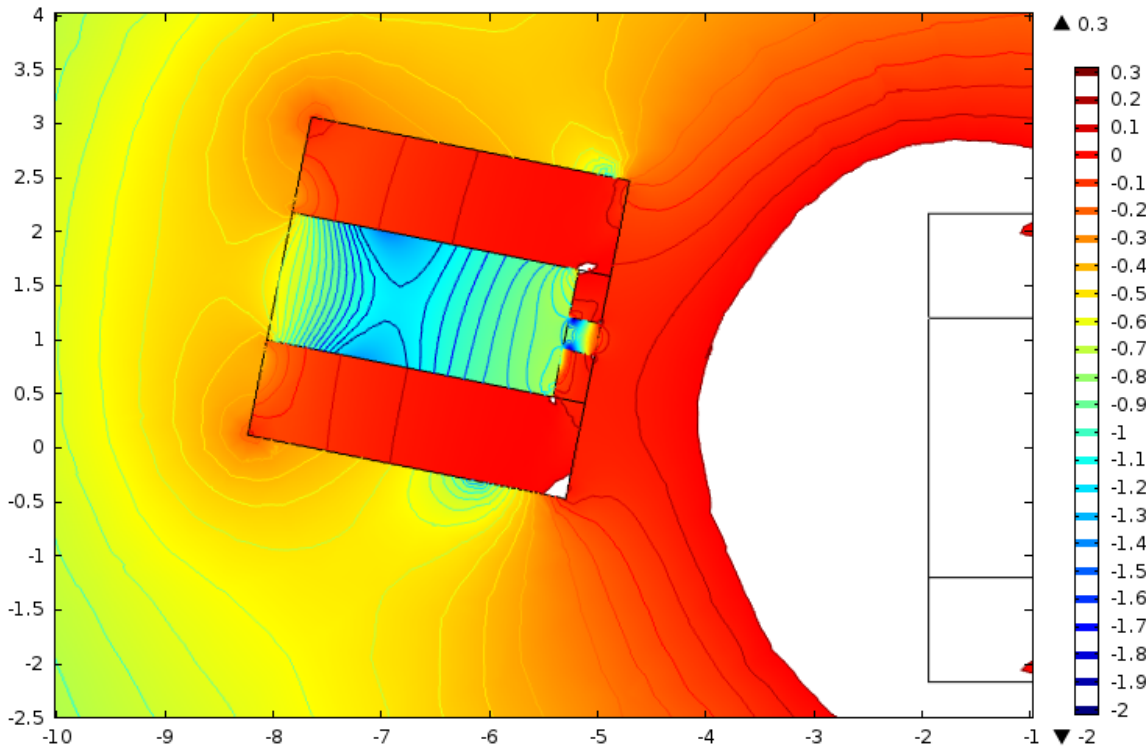


Fig. 7.  $\text{Log}_{10}$  of field with cylindrical shell of 0.6-m I.R., 3-m length & 90-cm thickness, with flange of 0.15-m I.R. and 30-cm length, displaced radially by 1 m at  $z = -5$  m and rotated  $11.3^\circ$  clockwise so that axis continues to point at  $r=0, z=0$ .  $M = 141$  tonnes. [Note: The solenoid axis is horizontal, instead of vertical as in preceding figures.]